Biological Structure Evaluation of 3-Methyl-4-Nitrophenol along with Molecular docking Visualization

S.Sindhuja[a,*], M. Karnan[a], R.Gayathri[b] and R.Elayaraja[c]

[a]PG& Research Department of Physics, Srimad Andavan Arts & Science College (Autonomous) (affiliated to Bharathidasan University), Trichy, Tamil Nadu, India.
[b]PG and Research Department of Physics, Cauvery College for Women(Autonomous)(affiliated to Bharathidasan University), Trichy, Tamil Nadu, India.
[c]Department of Physics, Sri Meenakshi Vidiyal Arts and Science College, Trichy, Tamil Nadu, India.
*ssindhujaphysics@gmail.com

Abstract

On 3-Methyl-4-Nitrophenol, X-ray crystallographic, FT-IR, FT-Raman, UV-Vis, DFT, MEP, and Molecular docking investigations are carried out (3M4NP). Docking tests using small molecules (3M4NP) with protein of relevance found because it is a strong molecule that attaches to arange of Human apolipoprotein C-II in dodecyl phosphocholine (PDB ID: 1SOH) protein. MEP assists the interactions between proteins and ligands. Molecular simulation Process are used to establish the optimized shape of the 3M4NP molecule. Spectral interpretation confirmed the existence of functional groups in 3M4NP crystal, which showed good agreement when compared to DFT simulations. UV analysis used to determine the transmittance of the formed crystal.

Keywords: 3M4NP, DFT, MESP, Reactivity, absorption, FMO, Docking

1. Introduction

Aromatic compounds are of interest to chemists, materials scientists, and medicinal chemists, and they have been intensively researched. They're used as bioactive natural chemicals, synthetic intermediates, gas adsorbents, sensor chemistry, and luminous materials, among other things. Phenol derivatives are frequently employed in medicinal treatments for chronic inflammation management. Phenol is a common intermediary in the manufacturing of products including herbicides, dyes, and rubber [1-4]. 4-Nitrophenol, also known as 4-hydroxynitrobenzene, is a phenolic molecule having a Nitro group opposite the hydroxyl group on the benzene ring. 4-nitrophenol exists in two polymorphs in its crystalline form. The α-form and β-form have colorless and yellow pillars that are unstable and stable at ambient temperature. 4-Nitrophenol is a byproduct of paracetamol production. Before being

acetylated with acetic anhydride, it is reduced to 4-aminophenol. 4-NP is a precursor used in the manufacture of phenetidine and acetophenetidine, as well as indicators and fungicide raw materials. This chemical is seldom found in the body. Human apolipoprotein A-I (apoA-I) is a high-density lipoprotein (HDL) protein with antiatherogenic characteristics that participates in reverse cholesterol transport (RCT). Lipoproteins with apolipoproteins that may be exchanged regulate the equilibrium of cholesterol and triglycerides in the erythrocytes and the brain. Apolipoproteins are important lipid mediators to structural components of lipoproteins. Because of their detergent-like qualities, can emulsify lipid or stay in a soluble lipid-free form in various stages of self-association. Unfortunately, these characteristics have made high-resolution structural investigations of cardioprotective high-density lipoproteins difficult (HDLs).

In the present study, optimized geometry,spectroscopic analysis and docking analysis were employed to ascertain the structural and biological qualities. The relationship of 3M4NP and Human apolipoprotein C-II in dodecyl phosphocholine (PDB ID: 1SOH) Autodock software has been used extensively to study protein (Autodock, Autogrid, Autotors copyright-1991-2000).

2. Experimental Details

3M4NP sample was obtained from a pharmaceutical company and utilized without additional purification. FTIR acquired on a Bruker IFS 66V spectrometer using the KBr pellet method with a resolution of 4.0 cm^{-1} in 4000–400 cm^{-1} bandwidth. The FT–Raman acquired in the excitation wavelength in the 4000–50 $cm^{-1.}$

3. Computational Details

To accomplish all simulations, the Gaussian 09 [05,06] program was employed. The optimal geometries were found to be at stationary points matching local minima with no imaginary frequencies using frequency investigations. The molecular electrostatic potential (MESP) Map was also used to analyze the molecule's reactive behavior. The molecule's linear polarizability and initial derivative were calculated using GAUSSIAN 09W at the same level of theor in order to show its nonlinear optical (NLO) activity. Furthermore, because of their connection chargesand frontier molecular orbital (FMO) studies were done.

4. Result and Discussion

4.1 Optimized geometry

3M4NP is a C1 point group symmetry molecule having 18 atoms and 48 normal modes of vibration. The experimental and most stable, optimal geometry parameters derived by the DFT approach are listed in Table 1. The biggest divergence between experimental and theoretical values in this investigation of the 3M4NP crystal appears in the bond length N1-O2, which is roughly 0.0366 in the HF. In DFT calculations, N1-O2 is roughly 0.0366.The minimal variations for the C3-C4 and C1-C2 bond lengths are 0.0002 HF and 0.0015 DFT, respectively. Similarly, the maximum deviation bond angles O1—N1—C3 and O1—N1—O2 in DFT are 1.17° and 1.06°, respectively, and 1.1° and 1.03° in HF. The Bond angle C4—C3—N1 has no difference between the experimental value and the HF theoretical analysis, although the smallest deviation in the DFT calculations is roughly 0.08°. The average discrepancy between experimental and theoretical C-C bond lengths is 0.0019° for HF and 0.008° for DFT. Similarly, the actual and theoretical C-C-C bond angles diverge by 0.07° in HF and 0.075° in DFT. Because the experimental data is connected to the solid-state structure and the measured data is gathered throughout the gasification process, the calculated geometrical parameters are much longer and shorter than the experimental [07] values, as shown in Table 1. The configuration structure of 3M4NP is shown in Fig. 1.

Table 1 Structural parameters of 3-Methyl-4-nitrophenol

Bond Distance	Exp[12]	HF	DFT	Bond Distance	Exp[12]	HF	DFT
O3—C6	1.351 (2)	1.3636	1.3856	C5—C4	1.367 (2)	1.3726	1.3832
C7—C6	1.390 (3)	1.3834	1.396	C5—C6	1.393 (3)	1.3875	1.3984
C7—C2	1.393 (2)	1.3935	1.4024	C1—C2	1.511 (3)	1.509	1.5095
C3—C4	1.394 (3)	1.3938	1.4045	N1—O1	1.215 (2)	1.2302	1.2721
C3—C2	1.404 (2)	1.3988	1.4145	N1—O2	1.236 (2)	1.2321	1.2726
C3—N1	1.450 (2)	1.4419	1.4557				

Bond Angle	Exp[12]	HF	DFT	Bond Angle	Exp[12]	HF	DFT
C6—C7—C2	122.19 (15)	121.81	121.86	C7—C2—C1	118.12 (16)	117.95	118.27
C4—C3—C2	122.34 (15)	121.81	121.66	C3—C2—C1	126.04 (16)	125.65	125.31
C4—C3—N1	116.23 (15)	116.23	116.31	O3—C6—C7	122.66 (15)	122.27	122.57
C2—C3—N1	121.42 (16)	121.95	122.02	O3—C6—C5	117.02 (16)	116.91	116.67
O2—N1—C3	118.28 (16)	118.34	118.37				

[a]For numbering of atom refer Fig. 1.

[*]Ref. [12].

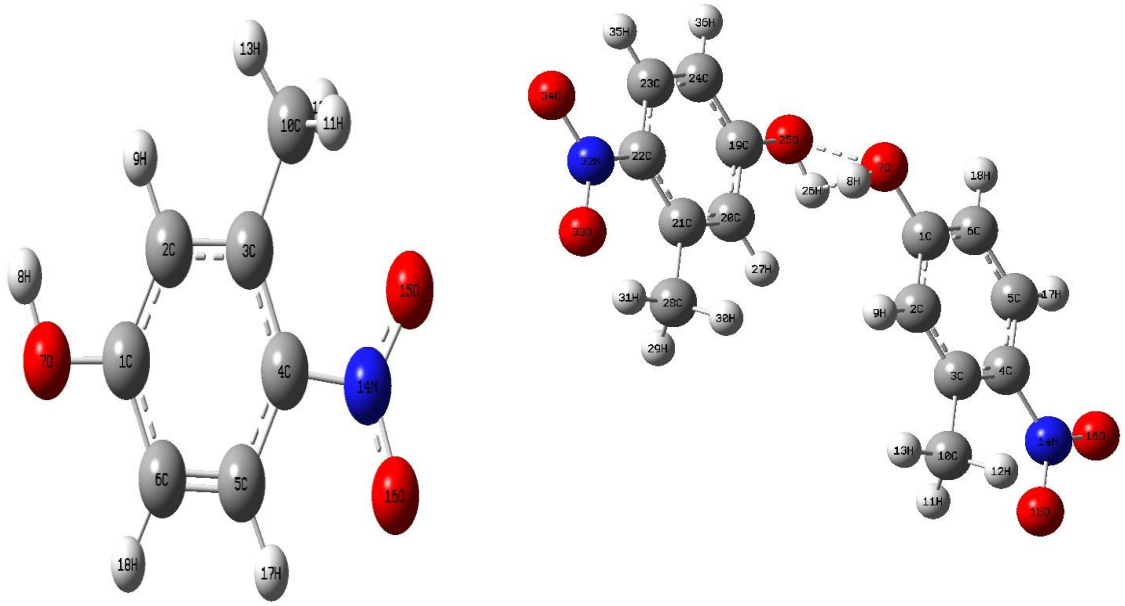

Fig. 1 Monomer and Dimer structure of 3-Methyl-4-nitrophenol

4.2 Vibrational assignments

Table 2 shows the comparison of the computed scaled values of harmonic vibrational frequencies to their experimental counterparts their spectra are shown in Figures 2 and 3, respectively.

4.2.1 Oxygen−Hydrogen vibrations

With an OH group connected to the first position of the benzene ring in 3M4NP, the OH stretching modes are indicated in the 3752-3430 cm^{-1} area [08, 09]. Experimentally, the signal appeared at 3282 cm^{-1} and was attributed to O-H stretching at 3827 cm^{-1}. With in deformation or rocking mode was anticipated by DFT simulations to occur around 1140 cm-1.

4.2.2 Carbon–Hydrogen vibrations

Stretching vibrations of 3076, 2947, and 2897 cm^{-1} were assigned to C-H stretching. At 3076 cm^{-1}, the υC-H modes was seen experimentally [10-12]. Out-of-plane deformation, also known as wagging vibration, has a volume of 539 cm^{-1}. According

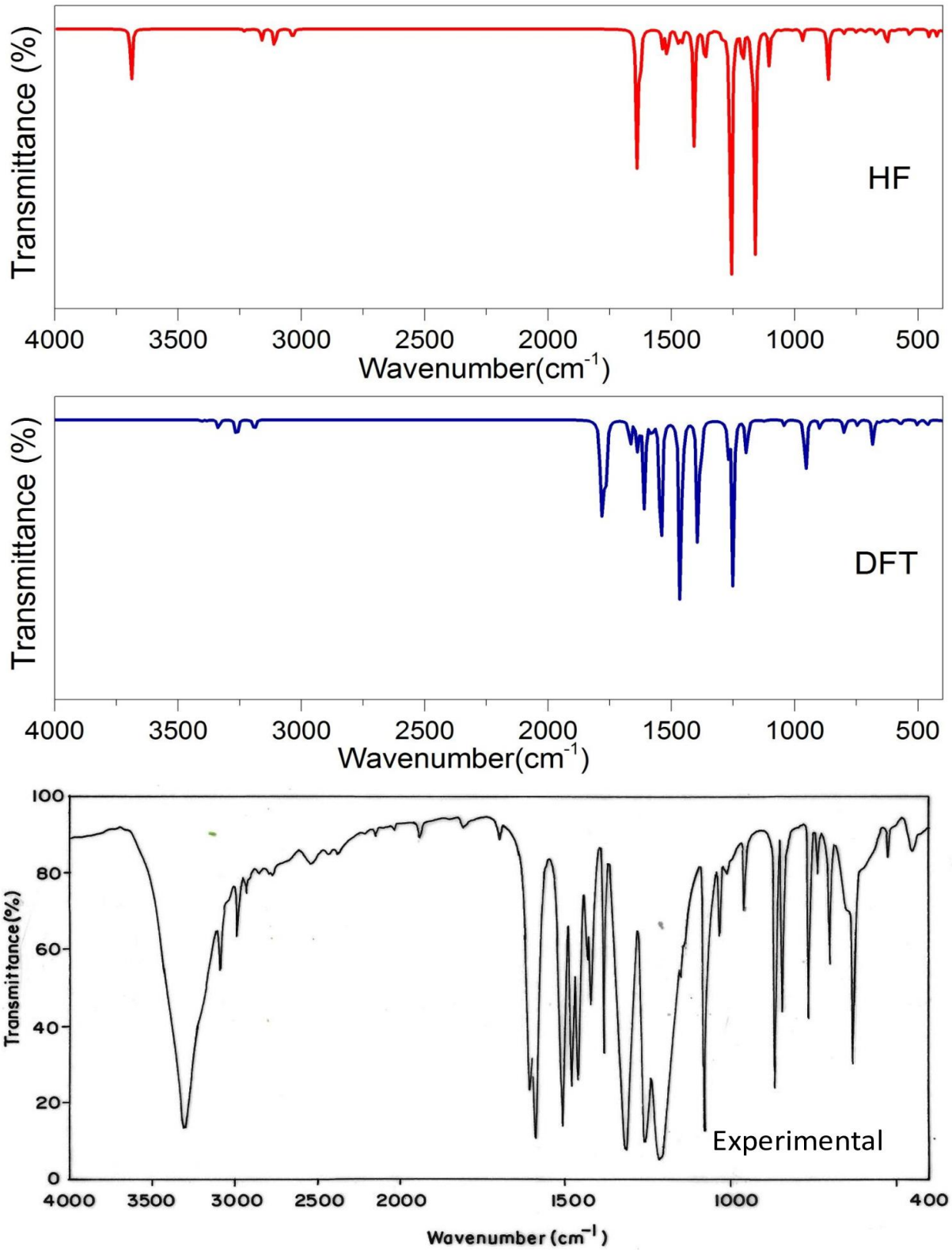

Fig. 2 Comparison between observed and calculated 3-Methyl-4Nitrophenol FTIR Spectra

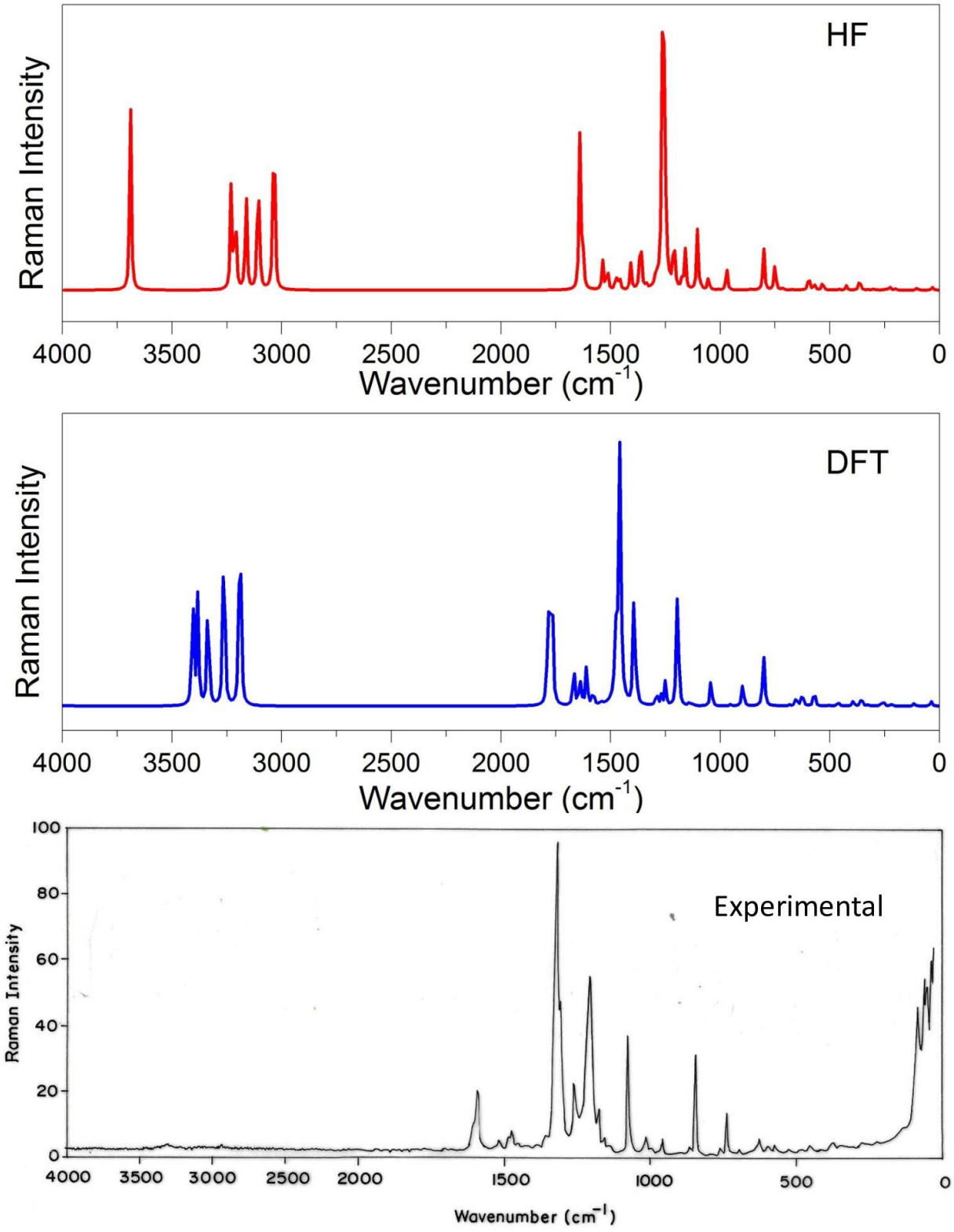

(a) Fig. 3 Comparison between observed and calculated 3-Methyl-4Nitrophenol FTRaman Spectra

Table 2 The probable assignments of 3-Methyl-4-nitrophenol

Symmetry Species C_1	Observed frequencies		Simulated frequencies (cm^{-1})				IR intensity		Raman intensity		Assignments with
	Wavenumber		Unscaled		Scaled		(KM/Mole)		(A^4/amu)		TED (%) among types of internal
	FTIR	FT-Raman	HF	B3LYP	HF	B3LYP	HF	B3LYP	HF	B3LYP	co-ordinates
A	3282	-	3945	3827	3290	3288	114.25	91.42	168.45	152.41	υOH(98)
A	3076	-	3327	3223	3089	3080	5.14	3	95.14	91.17	υCH(98)
A	2948	-	3307	3203	3005	3001	1.18	0.9	94.87	93.46	υCH(96)
A	2897	-	3285	3154	2915	2901	15.14	14.11	100.01	98.22	υCH(95)
A	2756	-	3225	3117	2768	2760	17.58	16.26	60.78	55.68	CH_3ss (90)
A	-	2879	3208	3110	2899	2887	6.21	5.04	70.89	65.86	CH_3ips (90)
A	2499	-	3142	3047	2514	2501	15.98	14.36	191..91	190.23	CH_3ops (92)
A	1596	1590	1698	1648	1604	1600	164.21	152.3	40.15	39.06	NO_2ass (89)
A	1576	-	1645	1631	1599	1580	129.47	128.36	52.78	51.42	υCC(90)
A	1512	1513	1587	1570	1525	1518	218.1	213.04	15.78	14.02	υCC(90)
A	1455	1471	1537	1520	1489	1475	39.47	38.49	7.45	8.62	υCC(89)
A	1442	-	1524	1496	1468	1450	37.74	36.01	1.28	1.29	υCC(89)
A	1405	-	1485	1476	1414	1409	9.24	8.45	7.89	7.17	υCC(88)
A	1371	-	1462	1452	1385	1375	47.89	41.21	4.89	4.61	CH_3ipb (81)
A	1307	-	1435	1421	1324	1311	5.02	4.3	14.78	13.04	NO_2ss (81)
A	-	1301	1408	1362	1310	1305	375.14	301.67	229.1	224.04	υCC(80)
A	1243	1239	1398	1357	1255	1247	29.47	28.75	33.78	32.49	CH_3sb (82)
A	1205	-	1372	1325	1219	1208	86.74	82.47	54.69	53.22	υCC(81)

A	-	1182	1303	1284	1199	1185	198.45	196.85	30.78	29.29	υCN(81)
A		1164	1245	1197	1188	1167	152.78	146.48	19.89	18.27	υCO(78)
A	-	1140	1211	1190	1158	1142	58.78	52.9	4.05	1.28	bOH (78)
A		1093	1197	1166	1100	1099	6.89	6.65	15.78	14.27	bCH(74)
A	1064	-	1124	1092	1085	1067	68.78	66.03	46.89	41.31	bCH(72)
A	-	1046	1095	1054	1061	1049	3.45	2.95	0.89	0.55	CH_3opb(72)
A	1012	-	1078	1034	1025	1020	2.78	2.62	8.15	7.89	bCH(72)
A	948	943	997	982	989	960	0.78	0.73	1.98	1.25	CH_3opr(70)
A	846	-	986	970	898	854	16.75	15.87	11.78	10.02	CH_3ipr(73)
A	820	831	863	857	838	835	24.78	21.39	14.78	13.67	Rtrigd(70)
A	-	725	854	852	731	727	43.79	42.82	0.89	0.21	Rasymd(70)
A	743	-	842	836	758	750	1.897	0.65	0.56	0.5	Rsymd(68)
A	692	683	795	753	712	703	12.178	11.1	0.79	0.77	NO_2sciss(68)
A	615	612	752	745	626	620	4.152	3.6	17.48	14.64	bCC(67)
A		563	691	687	598	565	10.789	9.33	0.78	0.36	NO_2wag(65)
A	538	-	620	631	549	542	17.489	16.15	0.41	0.61	bCN(66)
A		525	605	597	534	529	4.645	4.52	5.78	5.69	bCO(65)
A		517	571	567	525	520	0.7985	0.24	2.97	2.85	NO_2rock(65)
A		504	534	528	515	509	8.147	7.15	4.89	4.73	wωCH(64)
A	-	446	456	450	485	452	10.014	9.2	0.78	0.49	wωCH(61)
A	-	430	449	433	449	435	8.579	7.05	1.89	1.34	wωCH(61)
A	-	388	383	364	397	390	106.98	105.49	2.78	1.75	tRtrigd(59)
A	-	366	367	359	375	367	7.897	6.04	3.789	2.05	tRasymd(59)
A	-	323	334	325	356	331	0.9784	0.8	0.789	0.27	tRsymd(59)

A	-	300	307	292	307	305	4.127	3.42	1.078	0.97	wωCC(58)
A	-	272	287	244	289	275	4.9879	3.38	1.478	0.4	wωCN(60)
A	-	224	229	221	230	228	0.4798	0.15	1.024	1.02	wωCO(60)
A	-	206	214	197	219	207	11.049	0.47	0.78	0.55	wωOH(59)
A	-	114	117	102	126	120	0.989	0.82	0.784	0.72	NO_2twist(58)
A	-	83	58	40	100	98	0.782	0.35	1.048	0.94	CH_3twist(58)

to the calculation, they emerge at 3223, 3203, and 3154 cm^{-1}, respectively. The estimated values for CH_3 inplane deformation were 1093 cm^{-1} and 1064 cm^{-1}. In the ring CH stretching area, the vibrational spectra indicate six bands, There is also a distinct overlap between the various C-H stretching modes. Table 2 depicts the asymmetric and symmetric C-H stretching bands for the -CH3- group. The literature [13-15] also confirmed these allocations.**4.2.3. Carbon-Nitrogen vibration**

Because vibrations may mix in the Carbon-Nitrogen vibration frequency range, detecting C-N vibrations is difficult. It is responsible for the IR bands visible at 1182cm^{-1}. Sundaraganesan et al. [16] came at the same conclusion.

4.2.4 Carbon-Carbon vibrations

In cyclic alkanes, C-C stretching vibrations appear as faint bands. therefore they're only useful for structural research [17]. The IR bands at 1576, 1512, 1455, 1442, and 1402cm^{-1} for the title chemical were attributed to C-C vibrations associated with the C-C-H. As a result, it is appear as moderate width in our analysis[18].

4.2.5 Nitro group vibrations

Hydrogen bonding does not affect the asymmetric stretching vibrations of NO_2. The asymmetric stretching mode of the NO_2 group has been ascribed to the infrared and Raman bands at 1596 cm^{-1} [19, 20]. The symmetric mode of nitro group has been related to the dynamic link in the infrared around 1307 cm^{-1}.

4.2.6 CH_3 Vibrations

At 2756 cm^{-1}, the methylene group experiences stretching vibrations. The position of these bands changes by less than 10 cm^{-1} in wideband and restricted cyclic hydrocarbons[21]. The computed wavenumbers were 2940 and 2938 cm^{-1} , as shown in Table 2. Stretching of the C–H bond in CH_3 is less common than stretching of aromatic rings. CH_3 molecules have a mode in the range 2962–2872 cm^{-1} [18, 21]. In this investigation, CH_3 stretching vibrations were attributed to the IR bands detected at 2896 cm^{-1} and the FT–Raman bands recorded at 2879 cm^{-1}.

4.3 Mulliken Charges

Table 3 depicts the Mulliken electron density of 3M4NP. Carbon atom C3have the highest positive charges.The largest positive and negative Mulliken charges are found in carbon atom C3. Almost all H-atoms, including H8, H9, H11, H12, and H13, share the Mulliken charge plot plotted in Fig 4. Furthermore, O7 (-0.633044) and the nitrogen atom C10 (-1.299116) had the most negative charges. It demonstrates the presence of a methyl group as well as an O-H bonding system [22].

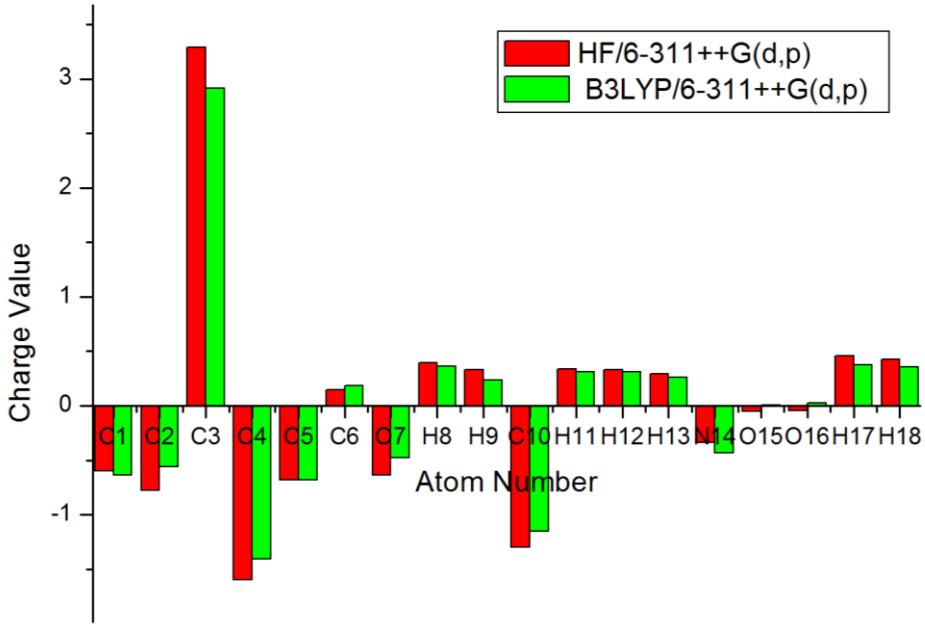

Fig. 4 Mulliken Plot of 3-Methyl - 4-nitrophenol

Table 3 The Mulliken charge for 3-Methyl-4-nitrophenol

Atoms	Atomic charges	
	HF/6-311++G(d,p)	B3LYP/6-311++G(d,p)
C1	-0.595562	-0.634510
C2	-0.774906	-0.560988
C3	3.290765	2.913746
C4	-1.597004	-1.403980
C5	-0.678188	-0.679259
C6	0.149709	0.183068

O7	-0.633044	-0.480138
H8	0.397041	0.362026
H9	0.330527	0.235949
C10	-1.299116	-1.149366
H11	0.336836	0.309124
H12	0.332264	0.310174
H13	0.292708	0.264098
N14	-0.338552	-0.435499
O15	-0.050824	0.005589
O16	-0.047304	0.023556
H17	0.457686	0.378601
H18	0.426963	0.357810

4.4 UV-Vis Spectral Analysis

TD-DFT calculations at the same level of theory were used to predict the absorption spectra, excitation energy, absorption wavelengths, and oscillator strengths, as well as the electronic transitions and their contributions. IEFPCM solvation model was used for the computations, which were done in a vacuum. Absorption occurs between 200 and 400 nm, as can be seen. At 346, 302, and 245 nm, three significant electronic transitions are expected. The greatest oscillator strength is computed at 346 nm (f = 0.0001) with an energy value of 3.5775eV, as shown in Table 4 and spectra given in Fig 5. Furthermore, the studied molecule exhibits outstanding transparency and low absorbance, as demonstrated experimentally [23,24]. This behaviour is considered to be a positive sign for NLO applications.

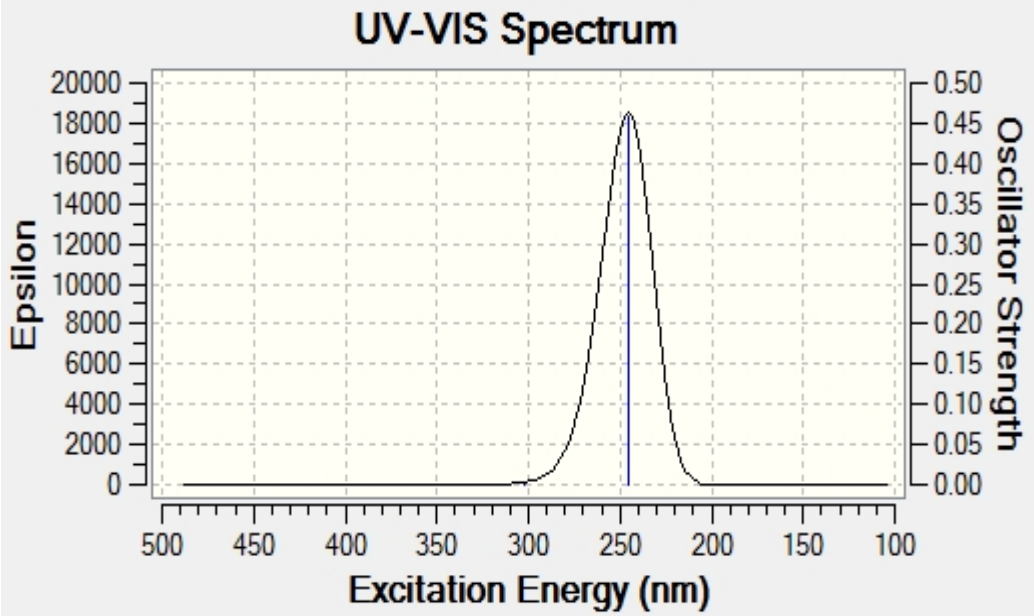

Fig. 5 Calculated UV-VIS spectrum of 3-Methyl-4Nitrophenol

4.5 First hyperpolarizability

The estimated polarizability values for the B3LYP and HF methods are $3.5x10^{-30}$ esu and $3.23x10^{-30}$ esu, respectively. The electric dipole moment (μ) for B3LYP was calculated to be 5.378 Debye, while it was calculated to be 5.214 Debye for HF levels. Our findings reveal that the first-order static hyperpolarizability values for the complex are 0.542 larger for B3LYP than for urea, a popular NLO material[25-26]. The molecule possesses a high degree of polarizability and hyperpolarizability, making it a good candidate for NLO materials.

4.6 Frontier Molecular orbital

The extraction and charting of HOMO and LUMO boundary orbitals are shown in Fig 6. The HOMO orbitals are typically found on the amino, carbonitrile, and phenyl groups, and are positioned at 7.1894eV. Despite this, except for the phenyl group, the LUMO orbitals at 2.5948 eV span. As previously stated, the H-L gap energy measures a molecule's chemical reactivity and kinetic stability [27-30]. As a result, soft molecules have a low gap energy, are highly polarizable, have a high chemical reactivity, and have a low kinetic stability. In this

scenario, the gap energy is calculated to be 4.5946eV the values are tabulated in Table 4 and 5,respectively.

Table 4 Electronic absorption spectral data of 3-Methyl-4--Nitrophenol

Excitation	CI expansion coefficient	Wave length (nm)	Oscillator strength (f)	Energy (eV)
H-7 -> L	-0.12599	346.57	0.0001	3.5775
H-4-> L	-0.21031			
H-3 -> L	0.60939			
H-3 -> L+9	0.11518			
H-3 -> L+2	-0.10209			
H-7 -> L	-0.12035	302.22	0.0005	4.1025
H-6-> L	-0.10563			
H-4 -> L	0.61418			
H-4 -> L+9	0.12651			
H-4->L+12	0.10418			
H-5 -> L	-0.14379	245.36	0.4572	5.0532
H -> L	0.62807			
H-1-> L	-0.18357			

Table 5 Molecular and Electronic Properties of 3-Methy-4-Nitrophenol.

Parameter	HF	B3LYP
Energy (E)	-647.789Hartree	–645.1723 Hartree
Dipole moment (μ)	5.214 debye	5.378 debye
Polarizability (α)	3.5×10^{-30} esu	3.23×10^{-30} esu
Anisotropy Polarizability (Δα)	4.7485×10^{-30} esu	4.7418×10^{-30} esu
Hyperpolarizapility (β^{vec})	3.651×10^{-30} esu	3.200×10^{-30} esu
μ X β	7.1047×10^{-30} esu	7.1478×10^{-30} esu
HOMO	7.2478eV	7.1894 eV
LUMO	2.4124eV	2.5948 eV
Energy gap (Eg)	4.8354eV	4.5946eV
Electronegativity (χ)	4.8301eV	4.8921eV
Chemical potential (μ)	-4.8301eV	-4.8921 eV
Chemical Hardness (η)	4.8354eV	4.5946eV
Softness (S)	0.2068eV	0.2176 eV
Electrophilicity index (ω)	7.9784eV	8.0289eV

The reactivity of the molecule is increased by this low number. The density of states (DOS) at the energy level is depicted in Fig 7. This finding supports the existence of tautomeric effects within the crystal lattice and suggests there are several intermolecular interactions present.

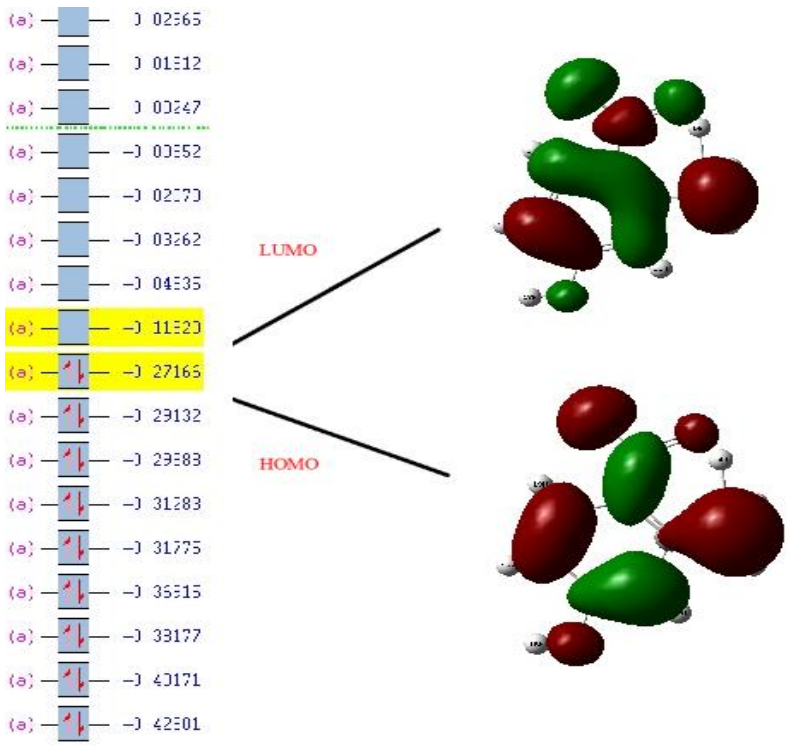

Fig. 6 Frontier molecular orbital for 3-Methyl-4-Nitrophenol

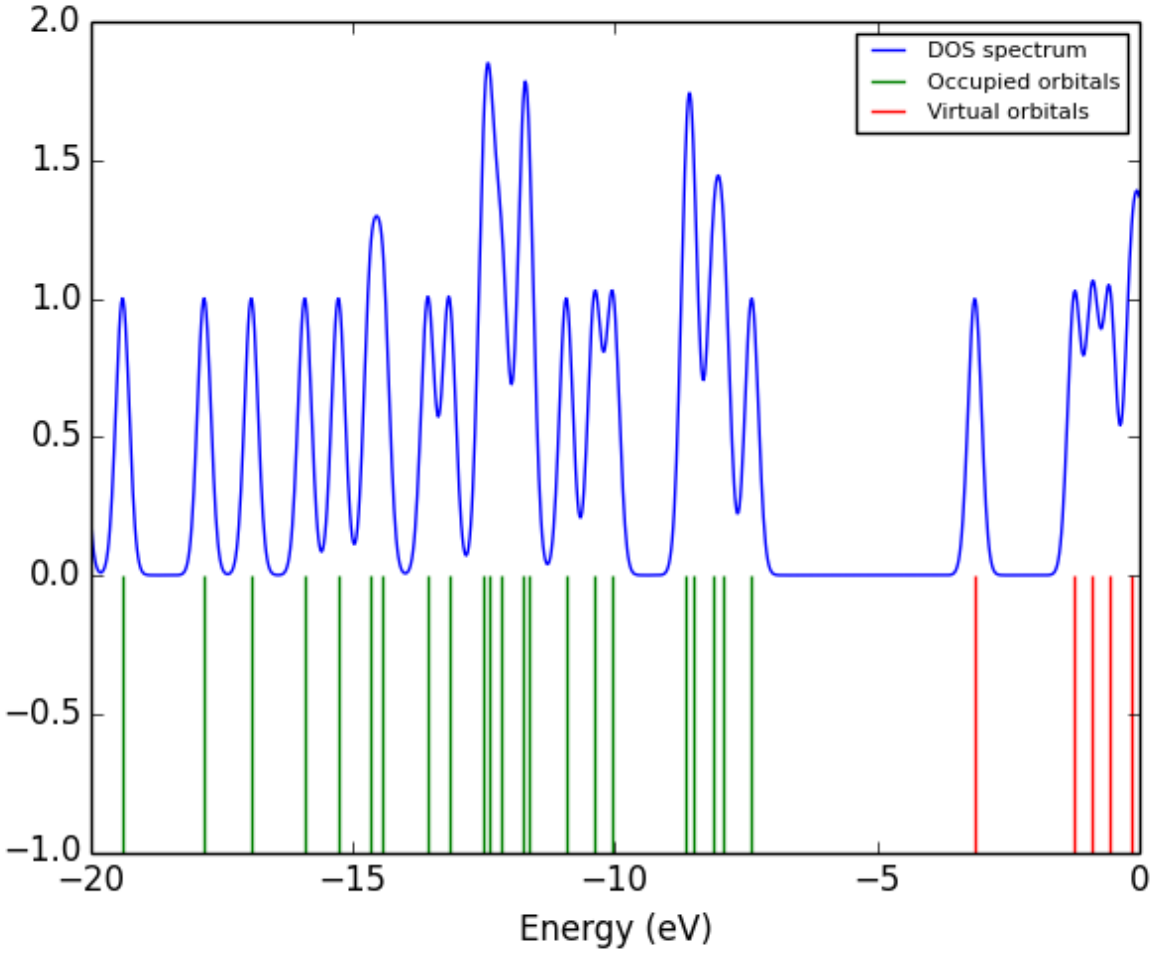

Fig. 7 DOS Spectra of 3-Methyl-4-Nitrophenol

4.7 Molecular electrostatic potential (MEP)

Fig 8 depicts the MEP surface, which was built at the same theoretical level. This approach provides a visual aid for seeing the researched compound's electrophilic and nucleophilic behavior [31]. Negative regions appear around the NO2 of the benzene ring, as seen in Fig. 8, which could be explained by tautomeric effects and their implications for Network with H-bonding. Positive zone, shown by the deepest blue hue, formed surrounding the ring's OH group, allowing strong hydrogen bonding to form. The electrophilic and nucleophilic behavior of the CO and NO_2, respectively, clearly demonstratethe occurrence of intermolecular interactions between molecules that make up the crystal packing.

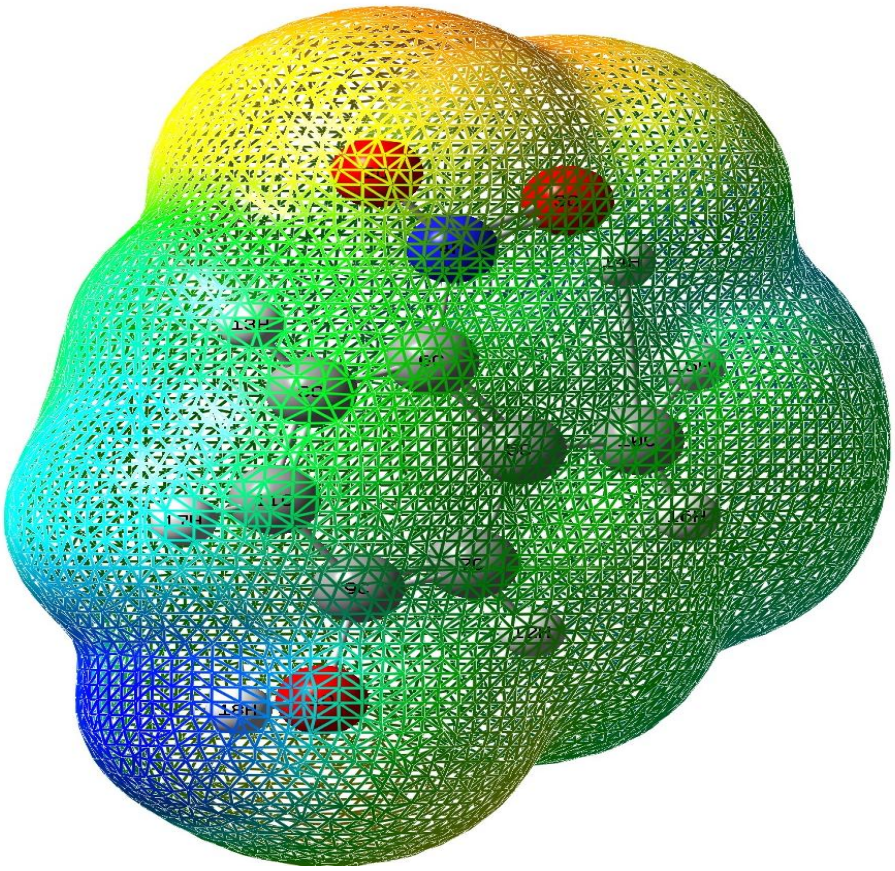

Fig. 8 MESP of 3-Methyl - 4-nitrophenol

4.8 Statistical properties

Using statistical keywords , the total energies and variations in total entropy of 3M4NP at room temperature are just marginally different[32-34]. The zero-point vibrational energy for the title chemical was calculated as 90.5039 kcal mol^{-1} and 90.340 kcal mol^{-1}, respectively, using structural optimization as shown in Table 6.

Table 6 Statistical properties of 3-Methyl-4-Nitrophenol

Parameters	**Values**	
	HF	**B3LYP**
Zero-point vibrational energy (kcal mol^{-1})	90.5039	90.340
Rotational Constants (GH_Z)		
A	2.25811	2.241
B	0.81057	0.801
C	0.60185	0.596
Thermal Energy (kcal mol^{-1})		
Total	96.111	90.023
Translation	0.889	0.889
Rotational	0.889	0.889
Vibrational	94.334	88.245
Entropy (cal mol^{-1} kelvin)		
Total	93.968	96.713
Translation	40.987	40.987
Rotational	30.057	30.125
Vibrational	22.924	25.601
Enthalpy (cal mol^{-1} kelvin)		
Total	33.772	36.388
Translation	2.981	2.981
Rotational	2.981	2.981
Vibrational	27.811	30.426

4.9 Fukui Indices

In conceptual density functional theory [35-37], Fukui functions calculated with total electrons present in the neutral, cation, and anion states of the examined molecule, respectively. Table 7 and the associated picture in Fig. 9 show the dual descriptor. Negative function values show that adding one electron to a molecule diminishes its electron density. On the other hand, the removal of an electron causes an increase in electron density. Positive f(r) values imply that the associated atoms are electrophilically vulnerable, whereas negative values suggest that they are nucleophilically vulnerable.

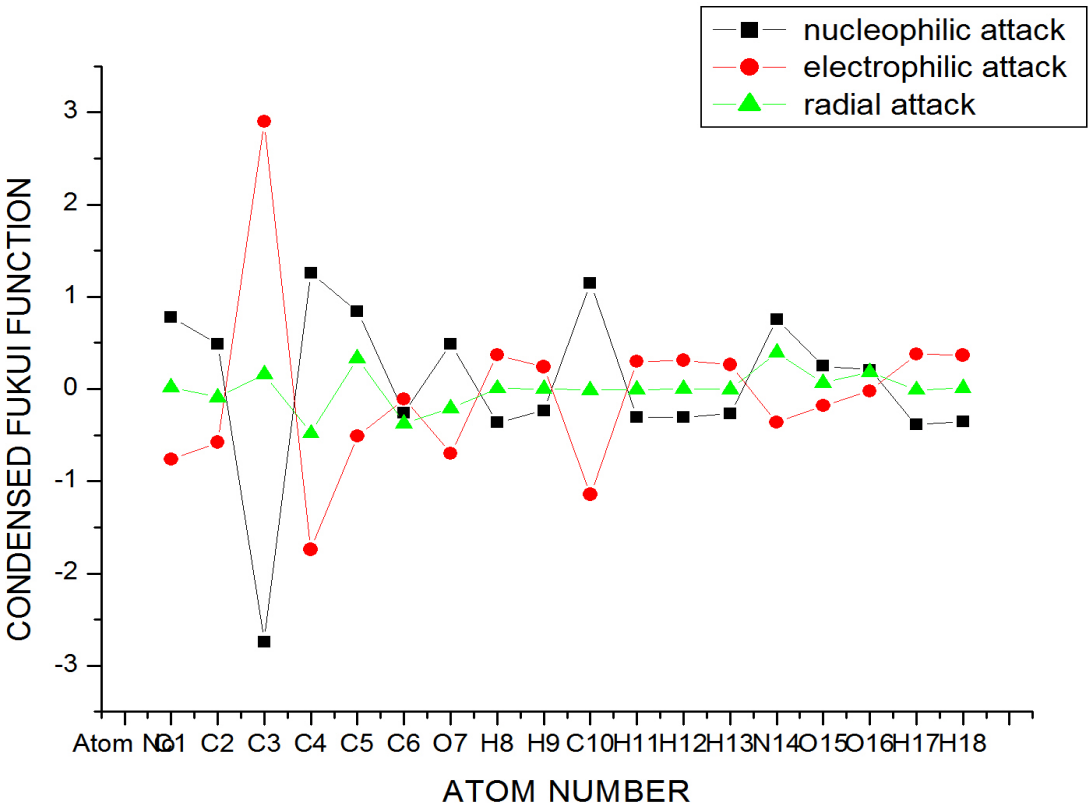

Fig. 9 Fukui function Plot of 3-Methyl-4-Nitrophenol

Table 7 The condensed fukui functional values of 3-Methyl-4-Nitrophenol.

Atom No	**N_k(N+1)**	**N_k(N-1)**	**N_k(N)**	**f_k^+**	**f_k^-**	**f_k^0**
C1	0.145520	0.125882	-0.634510	0.78003	-0.760392	0.01963
C2	-0.071700	0.018469	-0.560988	0.489288	-0.579457	-0.090169
C3	0.174481	0.015590	2.913746	-2.739265	2.898156	0.158891
C4	-0.144292	0.334788	-1.403980	1.259638	-1.738768	-0.47938
C5	0.165530	-0.168611	-0.679259	0.844789	-0.510648	0.334111
C6	-0.079797	0.292208	0.183068	-0.262865	-0.10914	-0.372005
O7	0.008135	0.218835	-0.480138	0.488273	-0.698973	-0.2107
H8	-0.000678	-0.007718	0.362026	-0.362704	0.369744	0.00704
H9	0.001264	-0.001937	0.235949	-0.234685	0.237886	0.003201
C10	-0.002016	0.007837	-1.149366	1.14735	-1.141529	-0.009853

H11	0.002221	0.009438	0.309124	-0.306903	0.299686	-0.007217
H12	0.004218	0.001629	0.310174	-0.305956	0.308545	0.002519
H13	-0.001272	0.001616	0.264098	-0.26537	0.262482	-0.002818
N14	0.319622	-0.074243	-0.435499	0.755121	-0.36125	0.393865
O15	0.253380	0.186537	0.005589	0.247791	-0.18094	0.066843
O16	0.231065	0.045394	0.023556	0.207509	-0.021838	0.185671
H17	-0.007915	0.001343	0.378601	-0.386516	0.377258	-0.009258
H18	0.002233	-0.007057	0.357810	-0.355577	0.364867	0.00929

4.10 Docking Studies

Molecular docking techniques help in the characterisation of the protein-ligand interaction by giving estimates of the ligand's binding shape as well as an energy rating methodology. Using automated molecular docking with the synthesised molecules, the best insilico conformation was determined. PASS (Prediction of Activity Spectra) is a web-based programme that predicts a variety of occurrences. A PASS test was performed on the chemical 3M4NP to predict its behaviour. Human apolipoprotein C-II was discovered in dodecyl phosphocholine by the PDB (http://www.pdb.org) [38]. (PDB ID: 1SOH). A Q-site Finder is used to hunt for potential binding sites of requested ligands in order to anticipate the ligand-binding site.

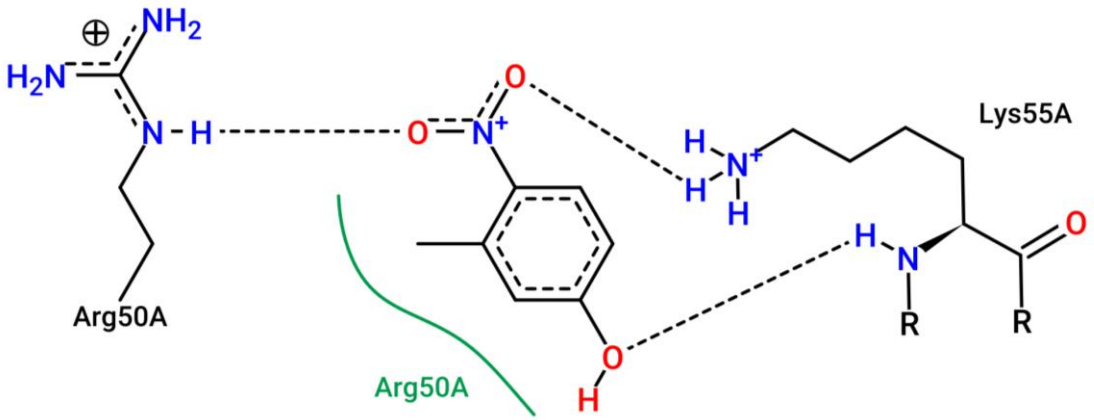

Fig.10 Poseview diagram of 3M4NP

Both compounds were docked using Autodock and stored in PDBQT format. The energy of the various docking possibilities compared, imitation structure with the minimum energy is judged to be the good. The energy of ligand-receptor interaction is -4.83 kcal/mol. The 3M4NP Poseview diagram and a hydrogen bond interaction of 3M4NP are shown in Fig. 10. The hydrogen bond between the NH of Arg50A and the 3M4NP Oxygen is 1.9Å, while the hydrogen bond between the NH of Lys55A and two Oxygens is 1.8Å and 2.1 Å. Fig 11 depicts it.

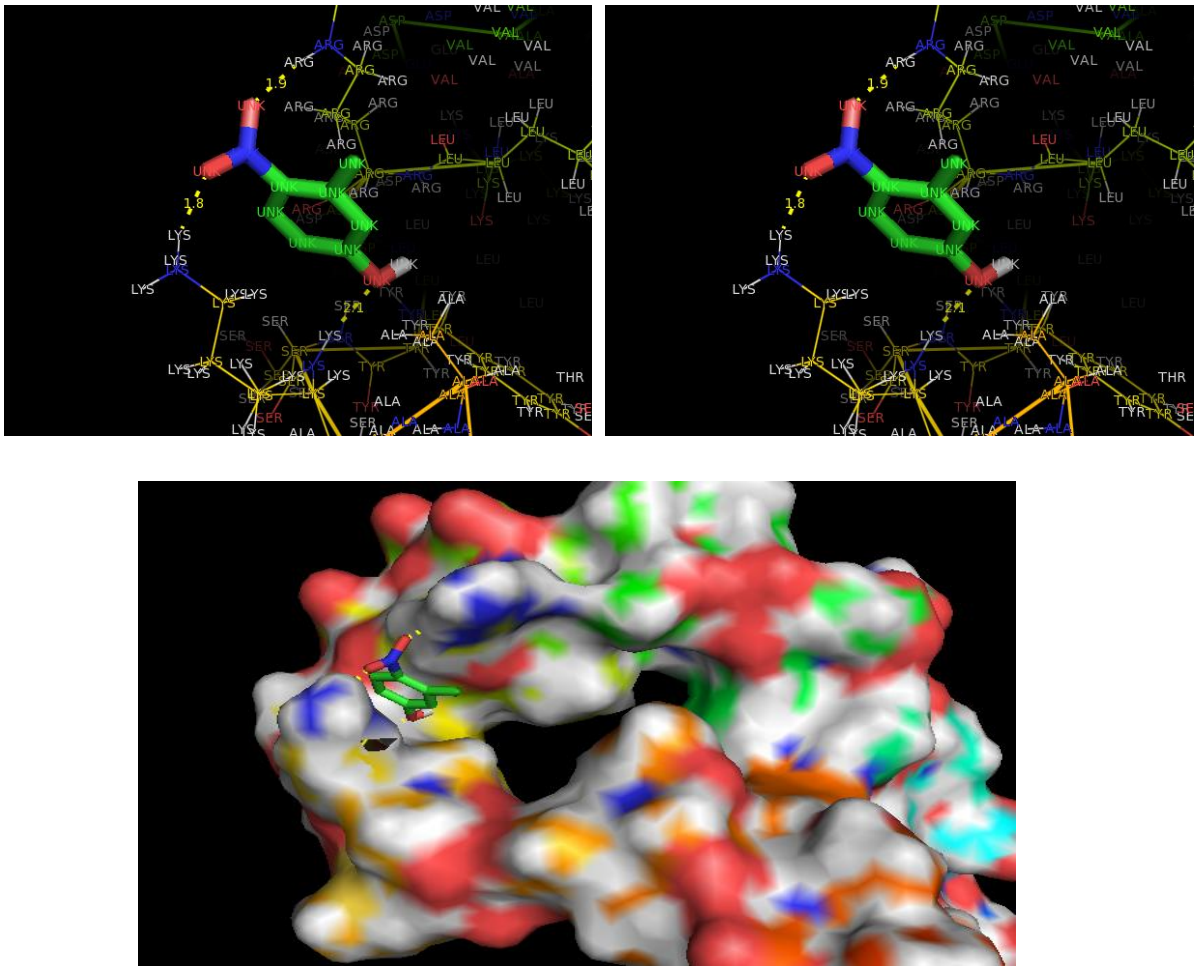

Fig.11 Biological assembly of 3M4NP

5. Conclusion

The molecular structure of 3M4NP was determined using density functional theory in this study (DFT). The expected frequency of vibrations matches the experimental data, according to spectra. LUMO, total energy values decreasing, whilst HOMO values are increasing, indicating that the more reactive molecule is engaging in electrophile reactions. Replacement causes new vibration modes and minor variations in stretching vibration, according to the vibrational investigation. During electrophilic, nucleophilic, radical, and dual descriptor assaults, Fukui indices are employed to determine the system's local reactive site. In Docking study, hydrogen bond between Arg50A's NH and the 3M4NP Oxygen is 1.9Å, while the hydrogen bonds between Lys55A's NH and two Oxygens are 1.8Å and 2.1Å.

Reference

1. Katritzky AR., Rccs CW, and Scrivcn EFV, Comprehensive Heterocyclic Chemistry II, Elsevier, Amsterdam, Netherlands, 1996.

2. Van Otterlo WAL, Ngidi EL,Kuzvidza S, Morgans GL, Moleele SS, and de Koning CB,Tetrahedron, 2005,vol. 61, no. 42, pp. 9996–10006.

3. Eichert T, Hauptmann S, and Speichcr A, The Chemistry of Heterocycles: Structure, Reactions, Synthesis and Applications, Wiley, Hoboken, NJ, USA, 2004, 2nd edition.

4. Lehnardt S, Massillon L, Follett et al P, Proceedings of the National Academy of Sciences, 2003, vol. 100, no. 14, pp. 8514–8519.

5. Frisch MJ, Trucks GW,Schlegel et al HB, Gaussian 09, Revision A.1, Gaussian, Inc., Wallingford, Conn, USA,2009.

6. Frisch A, Nielson AB, Holder AJ, GAUSSVIEW user manual, Gaussian, Inc., Pittsburgh, PA, 2000.

7. Mohsen Padervand,Hamed Heidarpou,Mahsa Goshadehzehn, SimaHajiahmadi , Environmental Technology & Innovation, 2021,Vol: 21 ,101212.

8. Arivazhagan M , Gayathri R , Spectrochimica Acta Part A: Molecular and Biomolecular Spectroscopy 116 (2013) 170–182.

9. Manimaran S, SambathKumar K, Gayathri R, Raja K, Rajkamal N ,Venkatachalapathy M , Ravichandran G ,Lourdu EdisonRaj C, Natural Products and Bioprospecting,2018.

10. Chaban GM and Gerber RB, Theoretical Chemistry Accounts, 2008,vol. 120, no. 1–3, pp. 273–279.

11. Sundaraganesan Nand Dominic Joshua B, Spectrochimica Acta—Part A, 2007,vol. 68, no. 3, pp. 771–777.

12. Arslan H and Demircan A, Molecular Simulation, 2008,vol. 34, no. 5, pp. 567–574.

13. Scott AP and Radom L, Journal of Physical Chemistry, 1996, vol. 100, no. 41, pp. 16502–16513.

14. Arslan H, Performance Analysis of Vibrational Frequencies, PAVF 1.0, Mersin, Turkey, 2007.

15. Arslan H, Algül Ö, and Dündar Y, Vibrational Spectroscopy, 2007, vol. 44, no. 2, pp. 248–255.

16. Sundaraganesan N, Ilakiamani S, Subramani P, and Joshua BD, Spectrochimica Acta—Part A, 2007,vol. 67, no. 3-4, pp. 628–635.

17. Mohan J, Organic Spectroscopy Principles and Applications, Narosa Publishing House, New Delhi, India, 2001.

18. Gunasekaran S , Thilak Kumar R, and Ponnusamy S, Spectrochimica Acta—Part A, 2006,vol. 65, no. 5, pp. 1041–1052.

19. Panicker CY, Varghese HT, George A, and Thomas PKV, European Journal of Chemistry, 2010,vol. 1, no. 3, pp. 173–178.

20. Arjunan V, Rani T, Mythili CV and Mohan S, European Journal of Chemistry, 2011,vol. 2, no. 1, pp. 70–76.

21. Frank Jensen, Introduction to Computational Chemistry, John wiley & sons, 2017.

22. Gayathri R, Journal of Molecular Structure (2018),1166 , 63-78.

23. Roohi H , Nowroozi AR, Anjomshoa E, Comput., Theor., Chem. (2011)965.

24. Chemla DS, Zysss J: Nonlinear Optical properties of Organic Molecules and Crystals Academic Press, Orlando, FL., 1987.

25. Bradshaw DS, Andrews DL, J. Nonlinear Opt. Phys. Mater., (2009) 18,285−299.

26. Cheng LT, Tam W, Stevenson SH , Meredith GR, Rikken G, Marder SR, J.Phys.Chem. (1991)95,10631–10643.

27. Muhammad Nadeem Arshad, Aisha Bibi, Tariq Mahmood, Abdullah M. Asiri, Khurshid Ayub, Molecules (2015) 20 ,5851-5874.

28. Gayathri R, Arivazhagan M, Spectrochimica Acta Part A: Molecular and Biomolecular Spectroscopy (2012)97, 311–325.

29. Anbarasan PM, Kumar PS, Vasudevan K, GovindanR, PrakasamA, and Geetha M, European Journal of Chemistry, 2011, vol. 2, no. 2, pp. 206–213.

30. Scrocco E and Tomasi J, Advances in Quantum Chemistry, 1978, vol. 11, pp. 115–193.

31. Luque FJ, López JM, and Orozco M, Theoretical Chemistry Accounts: Theory, Computation, and Modeling (Theoretica Chimica Acta), 2000,vol. 103, no. 3-4, pp. 343–345.

32. Gayathri R,Arivazhagan M,Spectrochimica Acta Part A (2011) 81, 242–250.

33. Geerlings P, De Proft F, and Langenaeker W, Chemical Reviews, 2003,vol. 103, no. 5, pp. 1793–1874.

34. Ghalla H, Issaoui N, Govindarajan M, Flakus HT, Jamroz MH, and Oujia B, Journal of Molecular Structure, 2014, vol. 1059, 132–143.

35. Fuentealba P, Pérez P, and Contreras R, The Journal of Chemical Physics, 2000,vol. 113, no. 7, Article ID 2544, 8 pages.

36. Otero N, Mandado M, and Mosquera RA, The Journal of Chemical Physics, 2007,vol. 126, no. 23, Article ID 234108, 6 pages.

37. Bultinck P, Fias , Alsenoy C van, Ayers PW, and Carbó-Dorca R, The Journal of Chemical Physics, 2007,vol. 127, no. 3, Article ID 034102, 11 pages, 43.

38. MacRaild CA, Howlett GJ, Gooley PR , (2004) Biochemistry 43: 8084-8093A.